d-band quantum well states in Ag(111) monolayer films; substrate-induced shifts

2008 J. Phys.: Condens. Matter 20 355004

(http://iopscience.iop.org/0953-8984/20/35/355004)

J. Phys.: Condens. Matter **20** (2008) 355004 (10pp) doi:10.1088/0953-8984/20/35/355004

d-band quantum well states in Ag(111) monolayer films; substrate-induced shifts

I Pletikosić[1], V Mikšić Trontl[1,2], M Milun[1], D Šokčević[3], R Brako[3] and P Pervan[1,4]

[1] Institute of Physics, Bijenička cesta 46, HR-10000 Zagreb, Croatia
[2] Faculty of Electrical Engineering and Computing, Unska 3, HR-10000 Zagreb, Croatia
[3] Ruđer Bošković Institute, Bijenička cesta 54, HR-10000 Zagreb, Croatia

E-mail: pervan@ifs.hr

Received 4 March 2008, in final form 10 July 2008
Published 1 August 2008
Online at stacks.iop.org/JPhysCM/20/355004

Abstract

We report a study of 4d electronic states in monolayer silver films grown on Pd(111), Ni(111), Mo(110) and Cu(100) surfaces studied by means of high-resolution angle-resolved photoemission spectroscopy (ARPES). The Ag-4d states, when measured in the surface Brillouin zone centre (SBZ), show substrate-dependent shifts. Density functional theory (DFT) calculations for a free-standing silver monolayer provide evidence that the observed shifts are not induced by lateral expansion, compression or distortion of the silver unit cell. Using the phase accumulation model we show that 4d-derived electronic states in silver monolayers can be described in terms of quantum well states and that the matching of the electron wavefunctions at the interface with the substrate is one of the important mechanisms that generates the Ag-4d energy shifts. The dispersion of the states around the SBZ centre is measured and discussed.

(Some figures in this article are in colour only in the electronic version)

1. Introduction

It is now well established that confinement of valence electrons in metallic films of nanometre and sub-nanometre thickness deposited on well-defined metallic and semiconductor surfaces can result in the formation of stationary states known as quantum well states (QWS) [1, 2]. The existence of these states is usually associated with discrete variation of a wide range of physical properties: density of states [3], work function [4], electron–phonon coupling [5–7], etc. Supported structures of reduced dimensionality provide a broad ground for manipulation of structural and electronic properties.

A particularly nice example of self-consistent balance between quantized size and electronic structure is the formation of ultrathin films and clusters of preferred dimensions [8]. Namely, the size of a nano-object (e.g. ultrathin film thickness) that causes confinement of the electronic system governs the energy distribution of the QWS, which in turn determines the total energy of the system and consequently its stability [8–11].

It has also been shown how the energy of QWS affects the strength of the interaction of electrons with phonon excitations, i.e. the electron–phonon coupling [5–7]. The shifts of QWS binding energy induced by the variation of the film thickness are associated with strong change in the electron–phonon coupling and, for some particular film thicknesses, the measured coupling constant is substantially bigger than the bulk value [5, 6]. Recently, the thickness dependence of QWS in Pb/Si(111) has been used to manipulate the Kondo effect in manganese phthalocyanine (MnPc) molecules [12]. Therefore, in order to tailor structural and electronic properties of supported nano-objects it appears to be rather important to properly predict binding energies of a particular set of QWS. In this respect knowledge about the influence of the substrate electronic structure on the energy of the QWS is very important.

An experimental study of d-derived QWS is more demanding in comparison with s–p QWS due to the large number of states within a narrow energy range, making the task of resolving individual QWS for films thicker than 2–3 monolayers (ML) rather difficult [13]. Still, significant progress has been made in understanding the development of electronic structure associated with the quantization of the d-band due to the size effect in ultrathin films [13–15]. The somewhat simpler electronic structure of monolayer films, with

[4] Author to whom any correspondence should be addressed.

respect to multilayers, provides easier access to their complete d-band electronic structure. Consequently, monolayer films provide an opportunity to make a more accurate study of different aspects of quantum size effects in supported quasi-2D systems, in particular the influence of the substrate.

Silver monolayer films are particularly suitable model systems. Due to its small free surface energy ($\gamma_{Ag} = 0.62$ J m^{-2}) silver wets most metal surfaces, forming well-defined 2D films. An early work by Shapiro *et al* [16, 17] explored the influence of the substrate on the d-valence band in silver monolayer films deposited on several low-index surfaces: Cu(111), Cu(100), Ni(111), Ni(100), Au(111) and Si(111)-7 × 7. The silver 4d-valence bands were found to have very similar dispersion to that previously observed in silver monolayers on Cu(100) studied by Tobin *et al* [18]. The general conclusion was that the Ag-4d bands show structure that is largely independent of the substrate, except for an overall shift in binding energy. More recent work of Feydt *et al* [19] was focused on the interface effects on d-derived QWS in monolayer films of Ag on W(110). The binding energies of the Ag-4d QWS were compared with the results obtained on some other low-index surfaces, with the conclusion that the binding energies and peak splitting of the 4d-derived QWS in silver monolayer films on different metal surfaces are very similar. These two seemingly conflicting conclusions are likely to be the consequence of insufficient energy resolution of the electron analysers used in collecting some of the experimental data, as well as possible problems in preparing adequately ordered monolayer films.

Recent impressive improvements in the energy resolution of electron energy analysers and in techniques for preparing surfaces and films have provided a solid ground to examine experimentally the d-derived QWS with much higher precision.

The 4d-QWS were recently studied in silver films deposited on low-index transition and noble-metal surfaces [13–15, 20–23]. Different methods have been used to analyse their evolution with film thickness and corresponding binding energies. The phase accumulation (PA) model was used to predict the energy of d-QWS in silver films on Fe(100) [13], W(110) [15] and V(100) [14]. The *ab initio* density functional calculations (DFT) applied to Ag/Pd(111) [23] and Ag/V(100) [24] systems successfully reproduced in-plane dispersion of d-QWS, but were less reliable in delivering correct binding energies due to the known tendency of DFT to place d-bands of noble metals too close to the Fermi energy [25]. A somewhat better agreement with experimental binding energies was found in modelling d-QWS in multilayer Ag films on V(100) within the tight-binding approximation [14].

In this paper we present high-resolution angularly resolved ultraviolet photoemission investigation of Ag-4d bands in monolayer films deposited on different low-index metal surfaces, combined with theoretical investigation of some model systems, with the main goal being to determine possible effects of different substrate surfaces on their binding energies and effective mass. To this end the substrate surfaces were selected so that the silver films exhibit basically identical structure. In such a way the variation in the electronic properties of the Ag films that might appear due to their structural differences is minimized. We have selected Pd(111), Mo(110), Ni(111) and Cu(100) as substrates on which silver forms monolayer films of hexagonal symmetry. However, due to the different unit cell parameters of the substrate surfaces the films show different levels of distortion. We will show that these structural distortions cannot explain the observed differences in the binding energies of the Ag-4d bands. We show also that, to a large extent, binding energies of the Ag-4d bands at $\overline{\Gamma}$ can be explained in terms of QWS.

2. Experimental and calculation details

The experiments were carried out in two separate ultrahigh vacuum (UHV) chambers with a base pressure in the range of 10^{-8} Pa. The chamber used for the structural investigation was equipped with a scanning tunnelling microscope (STM) and rear-view low-energy electron diffraction (LEED). For the photoemission experiments we used a UHV chamber equipped with Scienta SES-100 hemispherical analyser and a rear-view Auger electron spectroscopy (AES)/LEED system. HeI (21.22 eV) and NeI (16.85 eV, 16.67 eV) photons were used for excitation in the photoemission spectroscopy experiments. Measurements of dispersion along the high symmetry directions were performed by changing the polar angle of the sample.

In the photoemission chamber we could heat the sample up to 2000 K using indirect heating, and cool down to 50 K using the closed-loop He cold head. In the STM chamber heating was limited to 1200 K and no cooling was available. All photoemission spectra shown in this work were taken at a substrate temperature between 50 and 60 K while all STM experiments were performed at room temperature. Monocrystals of the four metals (Cu, Pd, Ni and Mo) were of nominal purity of 99.99% and were oriented with a precision of 0.1° and mechanically polished. Further preparation of the crystal surfaces was performed in a UHV environment.

Silver films were prepared by evaporation of pure silver from a resistively heated tungsten basket. The deposition rate was adjusted to be 0.2–1 ML min^{-1}.

The instrumental energy resolution in photoemission experiments was about 20 meV. The uncertainty in sample orientation was no bigger than 2° which transfers into less than 10 meV possible error in determining the binding energy (BE) of an electronic state in the Brillouin zone centre. In the case of weakly dispersing 4d bands, this error is even smaller.

The density functional calculations were performed using the DACAPO [26] computer program. We employed ultrasoft pseudopotentials corresponding to the Perdew–Wang (PW91) flavour of the generalized gradient approximation (GGA) functional. Although the GGA functional gives values for the lattice constant of the bulk metals which are slightly too large (which is a manifestation of the general tendency of the GGA to underbind) it is otherwise known to give very good results for the metallic systems considered in this paper, and is in that respect clearly superior to the simpler local density approximation (LDA). The electronic structure of clean

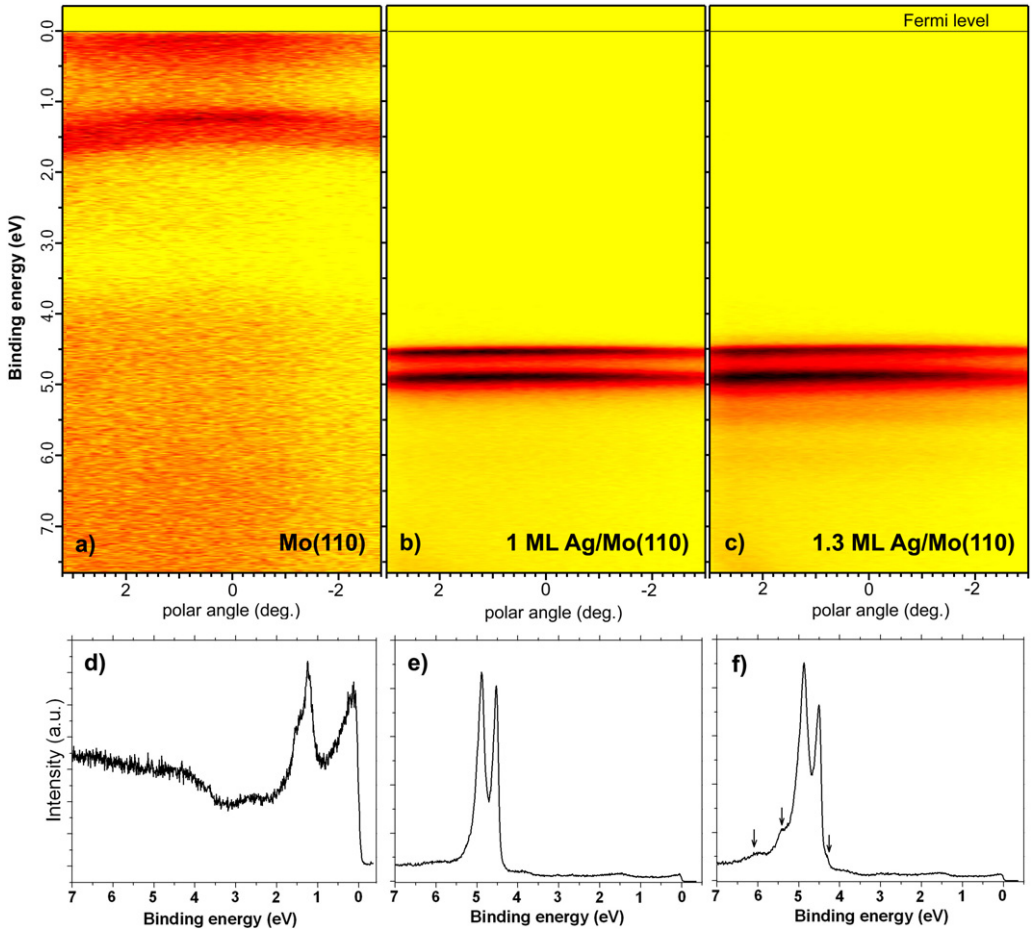

Figure 1. (a)–(c) Photoemission intensity maps as a function of initial-state electron binding energy and polar emission angle, proportional to the component of the electron momentum parallel to the surface, from (a) clean Mo(110), (b) 1 ML Ag/Mo(110) and (c) 1.3 ML Ag/M(110), recorded at a photon energy of 21.2 eV. The corresponding normal emission photoelectron energy spectra are shown below in panels (d)–(f).

surfaces was calculated by projecting the band structure of the bulk Kohn–Sham states. This is done by selecting a number of equidistant k-points in the direction perpendicular to the surface (i.e. the $\overline{\Gamma}$ point of the SBZ), and calculating the band structure for $k_{\|}$ along the high symmetry directions of the SBZ.

3. Experimental results

3.1. Silver monolayer structure

We used STM in combination with LEED measurements to characterize monolayer films on Pd(111) [23], Cu(100) [20] and Ni(111) [30] surfaces and to establish optimal experimental procedures for preparing well-ordered 1 ML Ag films on these substrate surfaces. The STM characterization of Ag films on Mo(110) was not done as our STM sample holder does not allow temperatures above 2000 K which are required for the cleaning of the molybdenum surface. In addition, photoemission from QWS was used for the accurate determination of the monolayer coverage. It is well established that s–p [27] and, in some favourable systems, d-QWS [14] can be efficiently used to monitor film thickness.

Both the growth and the structure of the silver monolayer on the four substrate surfaces have been well established [23, 28–31]. On Pd(111) silver grows epitaxially but slightly compressed [23] as a consequence of a mismatch of 4.8% between silver and palladium crystal lattices. On Cu(100) silver forms a slightly distorted hexagonal structure of c(2×10) symmetry [28]. The structural model proposed by Sprunger *et al* [28] shows that silver overlayer rows along the [011] direction are pseudomorphically placed with respect to the Cu atomic rows along the [011] direction. This geometrical constraint on much larger Ag atoms results in buckling of silver atoms with an amplitude of 0.42 Å, perpendicular to the surface. A silver monolayer on Ni(111) is known to produce hexagonal structure with bulk Ag(111) parameters. However, due to the large lattice mismatch (16%) with the nickel crystal lattice Ag forms the a moiré superstructure [29, 30]. The silver structure on Mo(110) is an undistorted hexagonal structure which exhibits Kurdjumov–Sachs orientation with respect to the underlying surface [31].

3.2. Photoemission results

As an example of photoemission spectra of silver monolayer films deposited on selected substrate surfaces figures 1(a)–(f) show photoemission spectra of a clean Mo(110) surface and the same surface covered by 1 and 1.3 ML silver films.

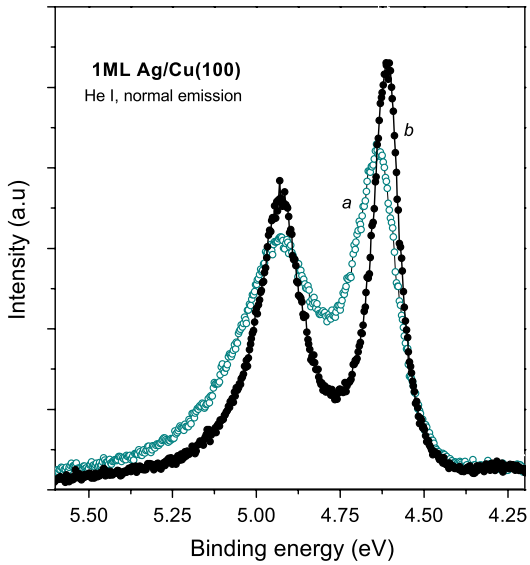

Figure 2. Normal emission photoelectron energy spectra showing the d-band QW peaks recorded at photon energy of 21.2 eV from monolayer silver films deposited on Cu(100). Spectrum (a) is from our previous work [20] and spectrum (b) from the present work. The figure points to the influence of the surface quality on both the line-shape and binding energy of a QWS.

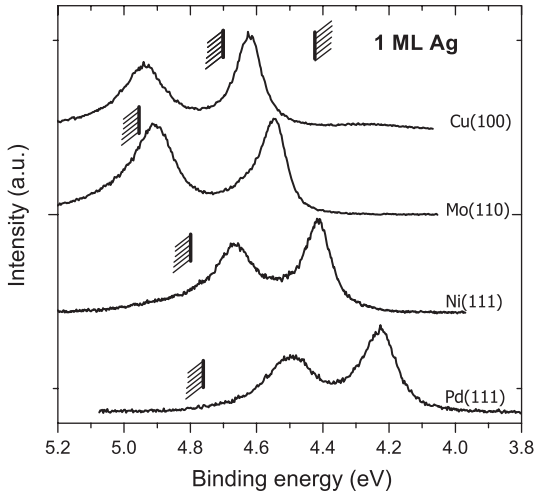

Figure 3. Normal emission photoelectron energy spectra of the d-band QWS recorded at a photon energy of 21.2 eV from monolayer silver films deposited on Cu(100), Mo(110), Ni(111) and Pd(111). The shaded thick marks indicate position of the projected energy band edges. For details see the text.

Figures 1(a)–(c) show photoemission intensity maps as a function of electron binding energy and polar emission angle (proportional to the component of the electron momentum parallel to the surface) obtained with photon energy of 21.2 eV. Panels (d), (e) and (f) show energy distribution curves, i.e. corresponding cuts of the spectra in panels (a)–(c), respectively, along the normal emission direction (zero polar angle). The photoemission intensity between the Fermi level and 2 eV binding energy is associated with the valence band electron states of molybdenum. The photoemission intensity corresponding to the silver monolayer appears at this photon energy as a characteristic doublet associated with the crystal field and spin–orbit split d-band of xz, yz symmetry [23]. It is important to point out that different photon energies can reveal different parts of the Ag-4d band due to their different excitation cross sections [14]. It has been also found that the relative photoemission intensity from $4d_{xz,yz}$ can depend on the polarization of the incident light [32].

Panel (f) in figure 1 shows the normal emission spectrum of a Mo(110) surface covered with more than 1 ML of silver. Compared to the 1 ML spectrum one can clearly notice additional peaks (indicated by arrows) characteristic for the second Ag layer [33]. These two spectra demonstrate the applicability of the photoemission spectroscopy of QWS for the calibration purposes. We have also noticed that sometimes, despite sharp LEED patterns suggesting well-ordered surfaces, the photoemission spectra of Ag-4d differ in their line-shape and to some extent even in their binding energies. In order to demonstrate this, in figure 2 we compare two photoemission spectra of Ag-4d taken from 1 ML Ag/Cu(100). Spectrum (a) is from our previous work [20] and (b) from this work. The two experiments were performed under very similar instrumental conditions and somewhat different monolayer preparation procedures. Obviously, spectrum (b) corresponds to a better-ordered silver film. Figure 2 carries two messages: (i) the quality of the film can affect the peak position of d-QWS and (ii) the line-shape and the peak positions of the d-QWS can be useful in estimating the quality of the film.

Figure 3 shows a narrow energy range of normal emission spectra of the 1 ML Ag films deposited on Pd(111), Ni(111), Mo(110) and Cu(100) surfaces. The shaded thick marks indicate the position of the projected energy band edges. The top and bottom of the gap are indicated only for the Cu(100) surface while for the other substrate surfaces only the bottom of the gap is shown as the top is out of range. The binding energies of the doublets are determined by fitting Lorentzian functions. In such a way the position of the maxima within the spectrum and relative separation between the peaks was determined with a precision between 1 and 2 meV. The energies of the photoemission maxima are as follows: Pd(111) (4.22 eV, 4.48 eV); Ni(111) (4.42 eV, 4.67 eV); Mo(110) (4.56 eV, 4.90 eV) and Cu(100) (4.60 eV, 4.92 eV).

From figure 3 it can be seen that there is a considerable energy difference (400 meV) between the doublet binding energies of the silver monolayer on the Pd(111) and Cu(100) surfaces. In addition the peak splitting of the doublet of 1 ML films on the Pd and Ni surfaces (260 meV and 250 meV, respectively) is clearly different from the Mo and Cu substrates (340 and 320 meV). It appears as if the peak splitting generally increases with increasing binding energy of the doublet.

Figure 4 shows four sets of dispersion curves for the Ag-$4d_{xz,yz}$ doublet around the centre of the Brillouin zone along the $\overline{\Gamma} - \overline{M}$ high symmetry line. The characteristic features are: (i) the dispersion of the bands is negative with a slight variation of the effective mass between the four substrate surfaces, (ii) for three substrate surfaces the band at higher binding energy shows stronger dispersion. The smallest effective mass of the topmost band (2.0) was measured in the monolayer film

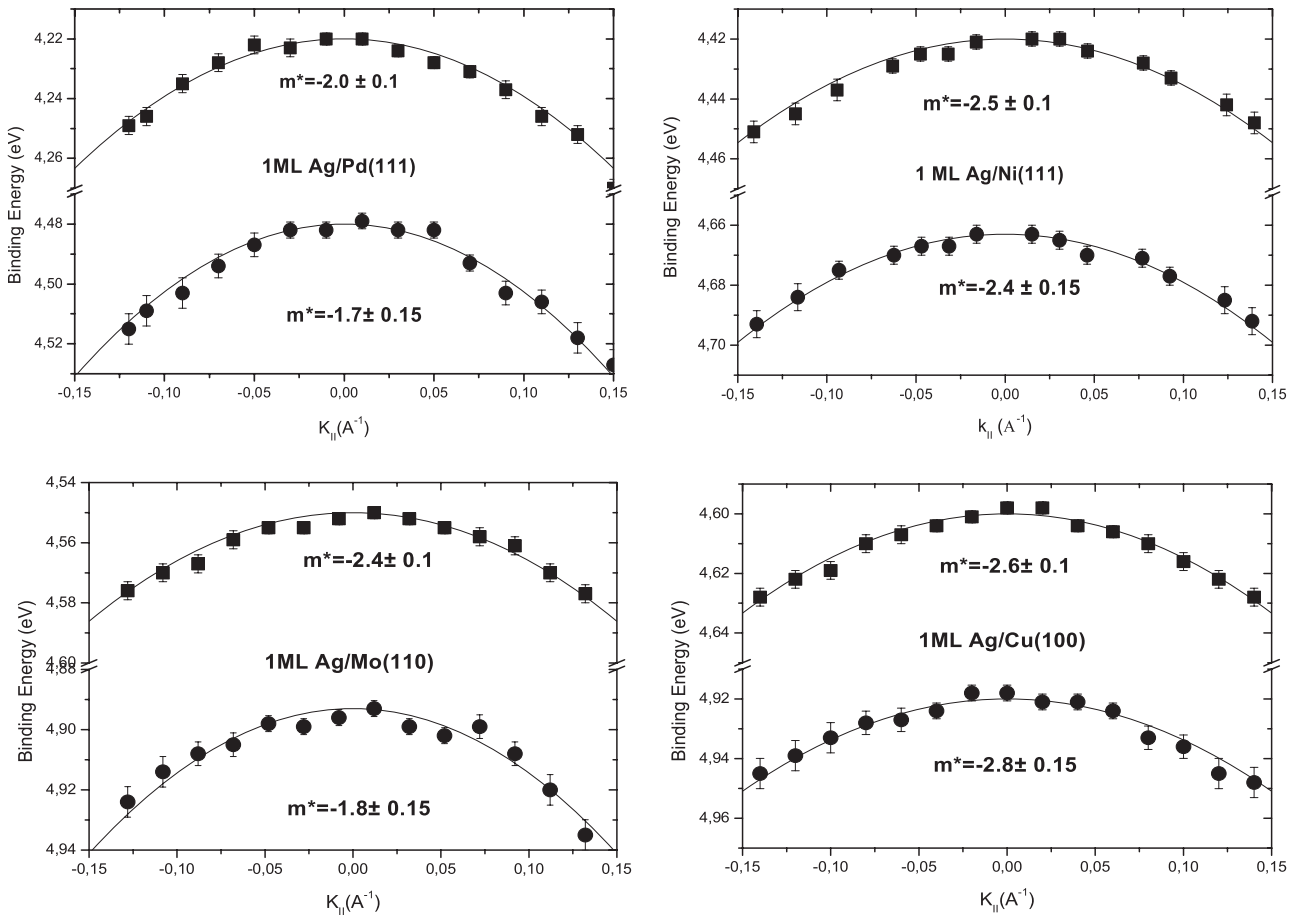

Figure 4. The dispersion of the QWS shown in figure 3 along the $\overline{\Gamma} - \overline{\mathrm{M}}$ high symmetry line. Effective masses $m^* = m/m_o$(m_o is the mass of a free electron) are indicated in the figure.

on the Pd(111) surface, somewhat smaller than on the other three surfaces (2.4–2.6).

4. Discussion

As figure 3 clearly shows, the silver monolayer films deposited on the four substrate surfaces exhibit a substantial difference in their $4d_{xz,yz}$ band binding energy. The leading peak of the doublet is nearly 400 meV closer to the Fermi level in silver film on the Pd(111) surface than on Cu(100). The overall influence of the substrate surface on the $4d_{xz,yz}$ band binding energy is shown to be even stronger when the data on Ag/Ta(110) [22] are taken into account. Namely, the leading peak of the doublet in a silver monolayer deposited on Ta(110) is found at 4.80 eV below the Fermi level, making the binding energy difference as big as 600 meV. Figure 3 also suggests that the doublet splitting depends on the substrate surface and generally increases with the binding energy of the doublet. The doublet splitting in the silver films on the Mo (Cu) surface is 90 meV (70 meV) bigger than on the Ni substrate. This general trend is additionally supported by recent photoemission measurements from monolayer silver films on W(110) [19] and Ta(110) [22]. The peak splitting of 400 meV was measured in the Ag/W(110) system where the binding energy of the leading peak of the doublet was 4.60 eV [19]. The largest peak splitting has been measured in a silver monolayer film on the Ta(110) surface (490 meV) [22]. However, the 260 meV splitting measured in the silver monolayer film on Pd(111) is clearly out of this simple trend.

As we have already pointed out, the properties of the 4d bands in silver films deposited on various substrate surfaces have been calculated, with different degrees of success, using TB and *ab initio* DFT methods. The DFT is the preferred method for modelling such systems, yet in cases of incommensurate or commensurate structures with a large periodicity they require prohibitively large unit cells and the method is not feasible for us.

In the following we explore the origins of the observed Ag-4d QWS energy differences by examining: (i) possible effects of structural differences in the Ag monolayers, induced by mismatch of unit cells of supporting surfaces and silver film, modelled by free-standing silver monolayers, and (ii) the influence of the wavefunction matching conditions at the interface using a phase accumulation model.

4.1. Free-standing silver monolayers

Based on previous calculations (Ag/V(100) [24] and Pd(111) [23]) we know that Ag-4d electronic structure within the floating silver monolayer is virtually unaffected by the

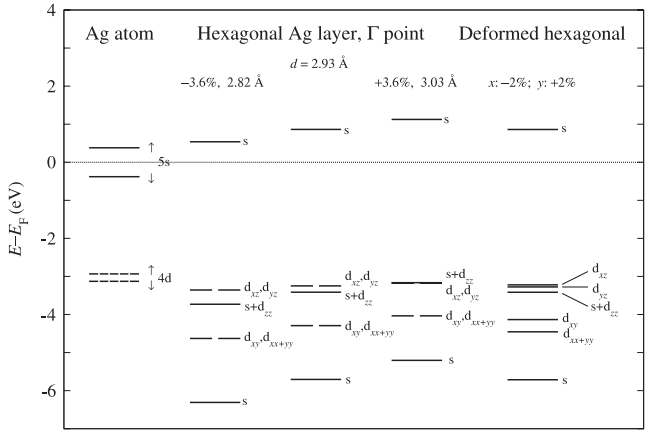

Figure 5. The calculated energies of electronic states of a free Ag atom (left) and of free-standing hexagonal Ag monolayers which are compressed by 3.6%, 0%, expanded by 3.6% and deformed by −2% and 2% in x and y directions, respectively (second to fifth columns). All values are for the surface Brillouin zone centre. The calculation illustrates the shift in energy and the reordering of d states due to the changes of the geometry of the layer.

interaction with the substrate, provided that, in the projected (E, k) phase space, the Ag-4d bands coincide with the substrate band gaps. Therefore, we believe the conclusions regarding possible effects of the structural distortions in the floating silver can be extended to the monolayer films on the four examined substrate surfaces.

For all systems studied, the silver monolayer forms a hexagonal structure distorted to a different extent, depending on the substrate surface. The silver monolayer forms an isotropically compressed (4.8%) hexagonal structure on the Pd(111) surface and a slightly strained (111) hexagonal structure (±2%) of c(2 × 10) symmetry on Cu(100). The silver monolayers on the Ni(111) and Mo(110) surfaces are less strained, although they have a more complex relationship with respect to the substrate structure parameters, as explained above.

In order to model effects of distortion of the silver monolayer crystal lattice with the main aim of determining the ordering of the 4d-states at $\overline{\Gamma}$ of the SBZ, we have calculated the electronic structure of two-dimensional hexagonal layers of Ag atoms at various values of the lattice constant (compression, expansion) and slightly in-plane distorted hexagonal lattice. One should bear in mind that the examined energy changes of the Ag-4d bands in the centre of the SBZ are not in simple correlation with the total energy of the monolayer film which increases upon any distortion of the unit cell.

There are two effects which split the degeneracy of the d-states manifold present in the atomic case: the crystal field, which is moderately long-ranged, and the delocalization effect (tunnelling of electrons between the atoms), which is of a shorter range. Figure 5 shows the binding energy of electron bands in the centre of the Brillouin zone of the free-standing hexagonal silver monolayer for three unit cells and crystal lattice contracted along the x-axis and expanded along the y-axis. The energies are compared to the binding energies of a free silver atom.

There are several trends connected to the change in size of the unit cell. The compression shifts the bands to higher binding energy while the expansion induces a shift toward the Fermi level. Accordingly, the binding energies of s bands, and to somewhat lesser extent d_{z^2} bands, depend strongly on compression/expansion. An expansion bigger than 3.6% leads to a change in the energy ordering of the $d_{xz,yz}$ and $s + d_{z^2}$ bands in a such a way that the band closest to the Fermi level is the $s + d_{z^2}$ band in the expanded layer and the $d_{xz,yz}$ band in the undisturbed layer. The total energy shift of $d_{xz,yz}$ due to the total compression/expansion of the unit cell of more than 7% is slightly bigger than 200 meV. Specifically, the *compression* of 3.6% leads to the shift of $d_{xz,yz}$ to higher binding energies by 125 meV. The *expansion* of 3.6% induces a shift of 100 meV to lower binding energies. The strain-induced changes in the electronic structure have been recently studied experimentally and theoretically on the Cu(100) surface [34]. That analysis as well as our own suggest that lateral compression of the crystal lattice shifts electron states to higher binding energies, affecting to a smaller extent the states closer to the Fermi level. Having in mind that the crystal lattice of the Ag film on Pd(111) is compressed, we would expect that this effect should shift the Ag-$4d_{xz,yz}$ states to higher binding energies when compared with states in films on other substrate surfaces, which is clearly not the case.

This indicates that effects of expansion and compression of silver monolayer film are not the prime source of the observed binding energy differences of the Ag-$4d_{xz,yz}$ states. The last column of figure 5 shows binding energies of states in the hexagonal lattice contracted along the x-axis and expanded along the y-axis which corresponds approximately to the geometry of the silver monolayer adsorbed on Cu(100) (without buckling which is present in the system). Due to the loss of symmetry, all degeneracy of the electronic levels is lifted. The 2% compression along the x direction and 2% expansion in the y direction introduces virtually no observable change in the energy of the Ag-$4d_{xz,yz}$ doublet. This is perhaps not surprising taking into account that this strained structure is only slightly different from the fully relaxed Ag(111) layer, e.g. their lateral densities differ by only 0.6% [28].

We have also explored possible effects of different adsorption sites in the moiré structure on the binding energy of the Ag $d_{xz,yz}$ bands. The calculated energy difference between Ag atoms in three-fold hollow sites and on top of a substrate atom is 100 meV, whereas the $4d_{xz,yz}$ band in an atom on top is closer to the Fermi level. Neglecting other possible effects, the moiré structure should shift the Ag-4d band slightly to a smaller binding energy with respect to the monolayer which consists of all atoms in three-fold hollow sites. However, the experimental result is just the opposite, the $4d_{xz,yz}$ band in the monolayer film on Pd(111) is 200 meV closer to the Fermi level than in the moiré film on Ni(111).

Taking into account the results of these model calculations we can conclude that the binding energy differences between the Ag-4d bands on the studied surfaces are not induced by the existing structural differences of the silver monolayers.

Recent DFT studies [24] of electronic states in a silver monolayer on V(100) shed some light on the possible

mechanisms that might cause the binding energy shifts reported in this work. Comparison of the states of the unsupported silver monolayer and the states of a 1 ML Ag film on V(100) clearly shows that the vanadium substrate induces a strong shift of the Ag-4d bands to higher binding energies. However, the calculation also showed that there is no significant hybridization of the 4d bands (apart from d_{z^2}) with the substrate. The shift to higher binding energies has been interpreted in terms of the width of the confining effective potential for the Ag-4d electrons; the localizing potential in a monolayer film on a vanadium substrate appears to be wider than for a free-standing Ag film. This indicates that, even if there are no significant hybridization effects between the silver film and the substrate, there can still be substantial *substrate-induced* energy shifts of the Ag bands due to the readjustment of the width of their localizing potential well. On the other hand, the effective width of the potential well depends on details of the electronic structure of both the substrate and overlayer through the matching conditions of the QWS wavefunction on the well boundaries. A phase shift of the wavefunction close to zero would result in effectively broader potential well compared to the case when the shift is close to $-\pi$ (see figure 10 in [2]) and accordingly position the QWS at higher binding energies.

As we have pointed out, no DFT studies of Ag films on Ni(111), Cu(100) or Mo(110) are available for the analysis of the localization of 4d electrons in monolayer films. For this reason we employed the phase accumulation (PA) model which provides a simple way to analyse binding energies of electrons trapped in a potential well in terms of total phase changes of the associated wavefunction [35].

4.2. Phase accumulation model analysis

The phase accumulation model is built on the simple fact that the total phase change of the wavefunction associated with an electron in an overlayer film localized by potential barriers at the interface (C) and the vacuum side (B) is a multiple of 2π [35]:

$$\Phi_C + \Phi_B + 2ka = 2n\pi \tag{1}$$

where Φ_C and Φ_B represent the phase change at the interface and vacuum side, respectively, and $2ka$ is the phase accumulated in traversing the monolayer film of thickness a. The model has been successfully applied in the analysis of many QWS of s–p and d symmetry. There is no doubt that, in general, the agreement produced by the model and experimental data increases with the film thickness (potential well width). However, the same model was successfully applied to the limit of zero film thickness, nicely predicting the energy of surface and image states [36]. The successful application of the model to the d-QWS is also encouraging [13–15]. In the Ag/Fe(100) system the model was used to recover the bulk dispersion of the Ag-4d bands along the Γ–L high symmetry line [13]. The d-QWS in multilayer silver films on V(100) were analysed in terms of the PA model, and qualitative and quantitative agreement was obtained [14].

Here, the prime interest in applying the PA model to monolayer films is to estimate how matching conditions of the silver 4d electron wavefunction at potential well boundaries, which is described through the phase shift Φ_C and Φ_B in (1), can affect their binding energy. For the four substrate surfaces we have generated Φ_C using (2):

$$\Phi_C = 2\arcsin\sqrt{\frac{E - E_L}{E_U - E_L}} - \pi \tag{2}$$

where E_U and E_L are the energies of the upper and lower boundaries of the substrate's total energy band gap, respectively. In this way the influence of the substrate on the binding energy of the stationary state of the film comes from the position and the width of the projected energy band gap. The projected band gaps had been calculated previously using different theoretical models for all four substrate surfaces (Cu(100) [37], Pd(111) [38, 23], Ni(111) [39] and Mo(110) [40]) but for reasons of consistency we have systematically recalculated the projected electron band structure on all four surfaces using *ab initio* DFT. Figure 6 shows an example of the calculated electronic structure of bulk copper and molybdenum, projected onto the (100) and (110) surface Brillouin zone, respectively. The positions of E_U and E_L are indicated in the figure. Table 1 summarizes the values of E_U and E_L for each substrate surface as obtained from our DFT calculation and compared with previous calculations. As can be seen from the table, there are no substantial discrepancies between the values of the band edges obtained in this work and in previous calculations. The exception is Pd(111), where the top of the s–p band in reference [38] is substantially closer to the Fermi level, but more recent calculations [41, 42] agree with our results. It is not straightforward to define the band gap of Ni(111) due to its spin dependence. However, recently Varykhalov *et al* [43] have experimentally determined, using QWS from multilayer Ag films, that the bottom and the top of the projected energy band gap on the Ni(111) surface are 2.6 eV and 4.8 eV, respectively.

Table 1. The energies of the top (E_U) and the bottom (E_L) of the projected band gaps in the $\overline{\Gamma}$ point of the SBZ for the corresponding surfaces. The values obtained from our and the calculations previously published (references shown in the table) are shown in parallel.

Surface	E_U (eV)	E_L (eV)	Reference
Pd(111)	2.81	4.77	This work
	2.65	4.21	[38]
Ni(111) up	2.10	4.45	This work
	2.18	4.36	[39]
Ni(111) down	2.65	4.79	This work
	2.36	4.72	[39]
Mo(110)	3.20	4.96	This work
	3.30	5.10	[40]
Cu(100)	4.38	4.75	This work
	4.57	5.00	[37]

The phase shift Φ_B at the vacuum side is

$$\Phi_B = \pi\left(\sqrt{\frac{3.4}{E_V - E}} - 1\right) \tag{3}$$

where E_V and E are in eV. The phase shift Φ_B was found to be almost constant for all substrate surfaces examined,

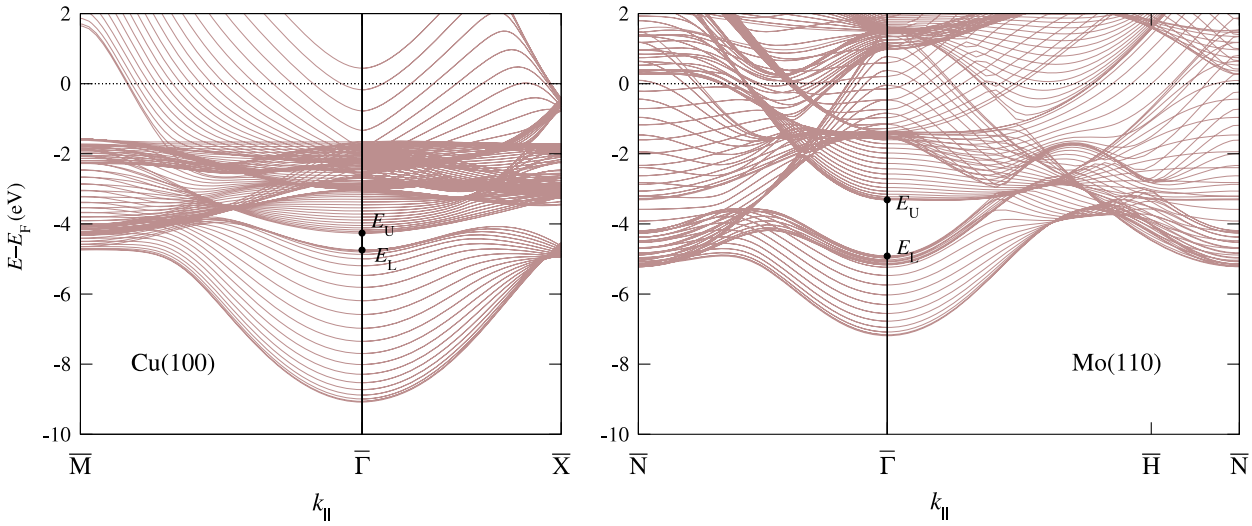

Figure 6. The electronic band structure of Cu(100) and Mo(110) surfaces, calculated by projection of bulk electronic states for several values of the component of the wavevector normal to the surface ($k_\perp$). The edges of the energy gap at the $\overline{\Gamma}$ points are denoted by dots.

which is due to the fact that the Ag-4d QWS are relatively deep-lying. In this energy range the slope of the localizing potential is constant or varies very slightly with the energy which causes only small changes in the phase shift. Finally, we have represented $k(E)$, for the respective Ag-4d bands, using the tight-binding model in the approximation of a linear atomic chain [44]:

$$2kd = 2kaN = 2\arccos\left(1 - \frac{2E}{E_{\mathrm{U}}^* - E_{\mathrm{L}}^*}\right)N \qquad (4)$$

where a is the layer spacing, N is the number of monolayers and E_{U}^* and E_{L}^* are the upper and the lower boundaries of the Ag-4d$\Lambda_{4,5}$ and Λ_6 bands [45].

Figure 7 shows the phase accumulation diagram where equation (1) is graphically solved for a silver monolayer on the studied surfaces: Pd(111), Ni(111), Mo(110) and Cu(100). Filled symbols indicate solution of the equation (1) for each substrate surface while the open symbols indicate experimentally determined energies of the QWS as obtained from figure 3.

We can draw several conclusions from figure 7. The phase accumulation model describes qualitatively correctly the relative position of the leading peaks of the Ag-4d QWS. It places Ag-QWS associated with the Cu(100) and Pd(111) surfaces to the highest and the lowest binding energy, respectively. The figure also clearly indicates why the peak splitting should generally increase with the binding energy. However, the model fails to explain why the binding energy of the 4d$_{xz,yz}$ band in a silver film on palladium is 200 meV closer to the Fermi level than on the nickel substrate.

Within the PA model the binding energies of QWS are determined by the phase changes on the potential well edges. For QWS at higher binding energies that is effectively reduced to the dependence of the phase change at the interface with the substrate. Previous DFT calculations show that the 4d-QWS in a silver monolayer on Pd(111) experience virtually no substrate influence, leaving the binding energies unchanged

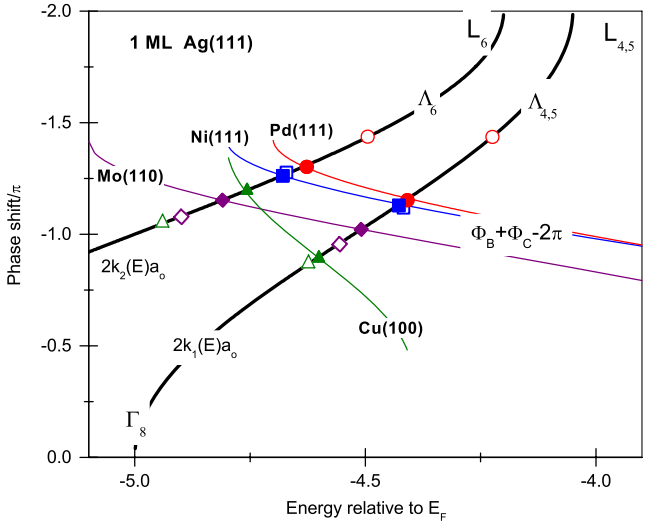

Figure 7. Graphical solution of the phase accumulation model equation (1) for d-band QWS in monolayer silver films on Pd(111), Ni(111), Mo(110) and Cu(100) surfaces. Thin lines represent the sum of the phase change at the vacuum and the interface barriers for a monolayer silver film on different substrates, as indicated in the figure. Thick lines are associated with silver bulk bands k(E) along the Γ–Λ–L high symmetry line. Open symbols indicate energies of QWS from figure 3 and solid symbols represent the solution of equation (1) for each substrate surface.

when compared to a free-standing Ag(111) layer. In the absence of any hybridization with the substrate it is obvious that the 4d$_{xz,yz}$ QWS experience the localizing potential of the same width as in a free-standing monolayer. That would imply that 4d-QWS in monolayer films on the other three substrate surfaces are localized within a wider localizing potential. Future *ab initio* calculations should resolve if this indeed might be the main origin of the observed peak shifts.

One of the strengths of the PA model in the analysis of Ag(111) monolayers is that it provides an intuitive explanation

for the increased QW peak splitting with the increase in the binding energy. Due to the combined actions of spin–orbit splitting and the crystal field effect the splitting between the d-QWS associated with $\Lambda_{4,5}$ and Λ_6 bands can change theoretically from 200 meV, which is the atom value of the spin–orbit splitting (L band edge), up to 800 meV, which corresponds to the energy difference between the Γ_8 and Γ_7 critical points in the centre of the bulk Brillouin zone. However, in some cases, the higher binding energy of the $4d_{xz,yz}$ band is not necessarily followed by a bigger peak splitting. This would be the case provided the phase change has the same energy dependence for all substrate surfaces, as is found for Ni(111) and Mo(110) surfaces for example. The total phase change is assumed to be the same in traversing the band gaps that may have different widths. It is therefore obvious that the phase shift will be a slowly varying function of energy in wide gaps and a fast varying function in narrow gaps. This has a clear consequence for the peak splitting: wide substrate band gaps should produce a bigger peak splitting than narrow gaps for comparable binding energies of QWS. Figure 7 suggests, in a rather exaggerated way, how the energy dependence of the phase shift could be the origin of the reduced splitting.

When discussing the Cu(100) substrate, one should bear in mind that the $4d_{xz,yz}$ split state at 4.90 eV binding energy overlaps with the projected electronic states of s–p symmetry (see figure 6). Although this might, at the first glance, complicate our simple PA analysis it has often been shown that hybridization gaps can be as efficient as projected energy gaps in localizing electrons in an overlayer film [14].

4.3. Dispersion around the SBZ centre

The Ag-4d bands in monolayer films show rather weak dispersion throughout the whole SBZ. The DFT calculations for Ag/Pd(111) [23] have shown that, due to moderate interaction with the substrate, the silver d-bands have virtually the same k-dependence as in unsupported monolayer film. Figure 4 shows the dispersion of the $4d_{xz,yz}$ bands around the centre of the Brillouin zone along the $\overline{\Gamma}$–$\overline{\mathrm{M}}$ high symmetry line. The fitting of the dispersion curves has shown that the bands around the zone centre have a simple-k^2 dependence. The fitting curves provide the effective mass $m^* = m/m_o$ where m_o is mass of a free electron. Only slight variation of the effective mass across the four substrates clearly shows that the interaction with supporting surface weakly affects the dispersion of the Ag-4d bands. Previous investigations of s–p QWS dispersion have shown that hybridization with substrate bands can affect their effective mass [46–49]. It has been demonstrated that the hybridization effects can cause strong anomalies in the dispersion of QWS [46, 49]]. Our experiments, which are focused on the d-states are not influenced by such effects. Namely, all topmost $4d_{xz,yz}$ bands of the spin–orbit doublet are positioned well inside the energy gap of the corresponding substrate and hybridization effects, if present at all, are probably very small. In addition, we could not observe any effect on the binding energy or dispersion of the Ag-4d band when crossing the band gap, as is clearly seen for s–p QW states in silver films on Ge(111) [50] and Si(111) [51]. Our results are more consistent with the experimental findings of Dil *et al* [52] who found a large difference in dispersion of the $6p_z$-QWS in ultrathin films of Pb and In on Si(111). It has been suggested that the large effective mass in Pb films is due to the localization of the electron states caused by structural effects. Namely, the structure of the Pb film is such that it induces lowering of the overlap of the $6p_z$ states in the direction parallel to the surface. A silver monolayer on Pd(111) is slightly compressed which, through the increased overlap of the orbitals, can induce an increase in the mobility of 4d electrons. On the other hand the increased corrugation through buckling in the moiré (on Ni(111) and Mo(110) surfaces) and (2×10) structures (on a Cu(100) surface) could be a reason for the increased localization. However, these structural differences in silver films are rather small and accordingly the differences in the dispersion are not as pronounced as in Pb and In films on Si(111) [52].

5. Summary

In this work we have presented photoemission measurements of the dispersion of the $4d_{xz,yz}$ electronic bands in silver monolayer films on Pd(111), Ni(111), Mo(110) and Cu(100), and interpreted the results using a combination of DFT calculations and the simple phase accumulation model. The Ag-4d band energies in the centre of the SBZ show substrate-dependent relative shifts. We have demonstrated, using the simple model of a free-standing silver atomic monolayer, that distortion from the ideal hexagonal structure that corresponds to the geometry of the adsorbed layer is not the origin of the observed differences in binding energy. Using the phase accumulation model we have shown that the 4d-derived electronic states in silver monolayers can be described in terms of QWS and that the matching conditions of the Ag-4d electron wavefunctions at the interface with the substrate might be one of the important mechanisms generating the Ag-4d energy dependence on substrate surfaces. In addition, the model clearly suggests why the Ag-4d band splitting should, in general, increase with increasing binding energy of the bands. However, this model fails to explain the energy difference of 200 meV between the $4d_{xz,yz}$ states in silver films on Ni(111) and Pd(111).

We also examined the dispersion of QWS around the SBZ centre. It appears as if the observed differences in the dispersion of Ag-4d around the Brillouin centre are more likely to be due to the slight structural differences in the silver film (corrugation) rather than to the interaction with the electron bands of the substrate surfaces.

Acknowledgments

The financial support of the Ministry of Science, Education and Sports of the Republic of Croatia through projects 035-0352828-2840 and 098-0352828-2836 is gratefully acknowledged.

References

[1] Chiang T-C 2000 *Surf. Sci. Rep.* **39** 181
[2] Milun M, Pervan P and Woodruff D P 2002 *Rep. Prog. Phys.* **65** 99
[3] Ortega J E, Himpsel F J, Mankey G J and Willis R F 1993 *Phys. Rev.* B **47** 1540
[4] Paggel J J, Wei C M, Chou M Y, Luh D-A, Miller T and Chiang T-C 2002 *Phys. Rev.* B **66** 233403
[5] Valla T, Kralj M, Šiber A, Milun M, Pervan P, Johnson P D and Woodruff D P 2000 *J. Phys.: Condens. Matter* **12** L477
[6] Luh D-A, Miller T, Paggel J J and Chiang T-C 2002 *Phys. Rev. Lett.* **88** 256802
[7] Mathias S, Wiesenmayer M, Aeschlimann M and Bauer M 2006 *Phys. Rev. Lett.* **97** 236809
[8] Luh D-A, Miller T, Paggel J J, Chou M Y and Chiang T-C 2001 *Science* **292** 1131
[9] Hupalo M, Kremmer S, Yeh V, Barbil-Bautista L and Tringides M C 2001 *Surf. Sci.* **493** 52
[10] Otero R, Vázquez de Parga A L and Miranda R 2002 *Phys. Rev.* B **66** 115401
[11] Upton M H, Wei C M, Chou M Y, Miller T and Chiang T-C 2004 *Phys. Rev. Lett.* **93** 26802
[12] Fu Y-S, Ji S-H, Chen X, Ma X-C, Wu R, Wang C-C, Duan W-H, Qiu X-H, Sun B, Zhang P, Jia J-F and Xue Q-K 2007 *Phys. Rev. Lett.* **99** 256601
[13] Luh D-A, Paggel J J, Miller T and Chiang T-C 2000 *Phys. Rev. Lett.* **84** 3410
[14] Kralj M, Pervan P, Milun M, Valla T, Johnson P D and Woodruff D P 2003 *Phys. Rev.* B **68** 245413
[15] Shikin A M, Rader O, Gudat W, Prudnikova G V and Adamchuk V K 2002 *Surf. Sci. Rev. Lett.* **9** 1375
[16] Shapiro A P, Wachs A L, Miller T and Chiang T-C 1985 *Solid State Commun.* **55** 1101
[17] Shapiro A P, Wachs A L, Hsieh T C, Miller T, John P and Chiang T-C 1986 *Phys. Rev.* B **34** 7425
[18] Tobin J G, Robey S W, Klebanoff L E and Shirley D A 1983 *Phys. Rev.* B **33** 2270
[19] Feydt J, Elbe A, Engelhard H, Meister G and Goldmann A 2000 *Surf. Sci.* **452** 33
[20] Mikšić Trontl V, Kralj M, Milun M and Pervan P 2004 *Surf. Sci.* **551** 125
[21] Hüger E and Osuch K 2004 *J. Electron Spectrosc. Relat. Phenom.* **141** 13
[22] Pivetta M, Patthey F and Schneider W-D 2003 *Surf. Sci.* **532–535** 58
[23] Mikšić Trontl V, Pletikosić I, Milun M, Pervan P, Lazić P, Šokéević D and Brako R 2005 *Phys. Rev.* B **72** 235418
[24] Lazić P, Crljen Ž and Brako R 2005 *Phys. Rev.* B **71** 155402
[25] Fuster G, Tyler J M, Brener N E, Callaway J and Bagayoko D 2003 *Phys. Rev.* B **42** 7322
[26] http://dcwww.camd.dtu.dk/campos/Dacapo/index.html
[27] Pagel J J, Miller T and Chiang T-C 1998 *Phys. Rev. Lett.* **81** 5632
[28] Sprunger P T, Lægsgaard E and Besenbacher F 1996 *Phys. Rev.* B **54** 8163
[29] Nakanishi S, Umezawa K, Yoshimura M and Ueda K 2000 *Phys. Rev.* B **62** 13136
[30] Mikšić Trontl V 2005 *PhD Thesis* University of Zagreb
[31] Gotoh Y and Yanokura E 1992 *Surf. Sci.* **269/270** 707
[32] Deisl C, Bertel E, Bürgener M, Meister G and Goldmann A 2005 *Phys. Rev.* B **72** 155433
[33] Pletikosić I *et al* 2008 in preparation
[34] Sekiba D, Yoshimoto Y, Nakatsuji K, Takagi Y, Iimori T, Doi S and Komori F 2007 *Phys. Rev.* B **75** 115404
[35] Smith N V, Brookes N B, Chang Y and Johnson P D 1994 *Phys. Rev.* B **49** 332
[36] Smith N V 1985 *Phys. Rev.* B **32** 3549
[37] Díaz Z and Muñoz M C 1994 *Phys. Rev.* B **50** 8824
[38] Louie S G 1978 *Phys. Rev. Lett.* **40** 1525
[39] Mittendorfer F, Eichler A and Hafner J 1999 *Surf. Sci.* **423** 1
[40] Jeong K, Gaylord R H and Kevan S D 1998 *Phys. Rev.* B **38** 10302
[41] MacDonald A H, Daams J M, Vosko S H and Koelling D D 1981 *Phys. Rev.* B **23** 6377
[42] Todorova M, Reuter K and Scheffler M 2004 *J. Phys. Chem.* B **108** 14477
[43] Varykhalov A, Shikin A M, Gudat W, Moras P, Grazioli C, Carbone C and Rader O 2005 *Phys. Rev. Lett.* **95** 247601
[44] Shikin A M, Vyalikh D V, Prudnikova G V and Adamchuk V K 2001 *Surf. Sci.* **487** 135
[45] See table I in Nelson J G, Kim S, Gignac W J, Williams R S, Tobin J G, Robey S W and Shirley D A 1985 *Phys. Rev.* B **32** 3465
[46] Johnson P D, Garrison K, Dong Q, Smith N V, Li D, Mattison J, Pearson J and Bader S D 1994 *Phys. Rev.* B **50** 8954
[47] Denese A, Arena D A and Bartynski R A 2001 *Prog. Surf. Sci.* **67** 249
[48] Matsuda I, Ohta T and Yeom H W 2002 *Phys. Rev.* B **65** 085327
[49] Upton M H, Miller T and Chiang T-C 2005 *Phys. Rev.* B **71** 033403
[50] Tang S-J, Basile L, Miller T and Chiang T-C 2004 *Phys. Rev. Lett.* **93** 216804
[51] Speer N J, Tang S-J, Miller T and Chiang T-C 2006 *Science* **314** 804
[52] Dil J H, Kim J W, Kampen Th, Horn K and Ettema A R H 2006 *Phys. Rev.* B **73** 161308